Journal of Applied Electrochemistry **32**: 497–504, 2002.

Study of the properties of a multi-component inhibitor used for water treatment in cooling circuits

N. OCHOA[1], G. BARIL[1], F. MORAN[2] and N. PÉBÈRE[1]*
[1]*Centre Interuniversitaire de Recherche et d'Ingénierie des Matériaux, UMR CNRS 5085, ENSIACET, 118 Route de Narbonne, 31077 Toulouse cedex 4, France*
[2]*Concorde Chimie, 118 Avenue du Docteur Rosenfeld, 93230 Romainville, France*
*(*author for correspondence, fax: +33 5 62 88 56 63, e-mail: npebere@ensct.fr)*

Received 9 October 2001; accepted in revised form 26 February 2002

Key words: carbon steel, EIS, fatty amines, inhibition, phosphonocarboxylic acid salts, XPS

Abstract

This work is devoted to the corrosion inhibition of a carbon steel in a 200 mg l^{-1} NaCl solution by an original multicomponent inhibitor: fatty amines in association with phosphonocarboxylic acid salts and a biocide at low dosage. Its principal advantage is the absence of toxicity and its biodegradability. Steady-state current–voltage curves were combined with electrochemical impedance measurements to characterize the inhibitive properties of each compound and to optimize the concentration of the compounds in the mixture. Phosphonocarboxylic acid salts were observed to act as an anodic inhibitor whereas mixed action was shown for fatty amines. The inhibitive efficiency was increased when the phosphonocarboxylic acid salt concentration was increased whereas for fatty amines an increase of the concentration did not improve corrosion inhibition. Optimal concentrations of fatty amines and phosphonocarboxylic acid salts were determined. X-ray photoelectron spectroscopy (XPS) was used to analyse the layer formed on the metal surface by the inhibitive mixture. The film was composed of an iron oxide/hydroxide mixture incorporating the organic compounds. The inhibitive molecules interact with the iron oxides.

1. Introduction

Water in cooling circuits is usually chemically processed to avoid formation of salt deposits and fouling by suspended solids and by microorganisms. The chemical reagents used to limit the scaling and fouling phenomena are mainly dispersing, complexing and sequestrating agents. These reagents are usually used in association with corrosion inhibitors. In the past, efficient corrosion treatments of carbon steels in cooling water systems were based on inorganic inhibitors such as chromates, nitrates, polyphosphates and zinc salts [1]. Today, the use of chromates and nitrites is restricted due to their high toxicity. In the case of zinc salts, their disposal in waste water at high levels has become unacceptable. Since the 1960s, more advanced treatments using organic compounds (e.g., phosphonates, polyacrylates, amines) have been proposed to improve corrosion protection, their principal advantage being their non-toxic nature. Nevertheless, high concentrations are necessary to obtain good inhibition. More recently, molybdate-based compounds have been considered as an alternative to chromate-based inhibitors [2, 3]. However, these compounds are of low commercial interest because they are very expensive. The prevention of corrosion and scaling in cooling systems is therefore usually achieved by organic mixtures. For many years, in our laboratory, comparative studies of the different possibilities of combining scaling and corrosion inhibitors has been undertaken to estimate their efficiency against the corrosion of carbon steel in neutral solutions [3–8].

As the inhibitive layers formed on the mild steel surface are relatively thin, their chemical composition can be determined by X-ray photoelectron spectroscopy [9–16]. Ashcraft et al. [9] studied the inhibitive film formed on a carbon steel in the presence of 2-phosphonobutane-1,2,4 tricarboxylic acid (PBTC). They found that PBTC is present only in the upper part of the film: Fe(II) ions are oxidized at the surface and transformed into hydrated iron oxide which reacts with PBTC. Olsson et al. [10, 11] have studied the adsorption of carboxylic acid-based inhibitors. They showed that the nature and the concentration of anions in the solution strongly influence the inhibitor efficiency. They suggested a competitive mechanism between the inhibitor, the hydroxyl ions and electrolyte anions [11]. Kálmán et al. [12, 13] studied the adsorption of hydroxyethane diphosphonic acid (HEDP) on differently oxidized surfaces by using surface analysis. They found that HEDP influenced the amount of iron oxyhydroxide on the surface. From XPS analysis, Fang et al. [14] confirmed the presence of the complex Fe[ATMP]$_2$ (ATMP: amino-trimethyl phosphonic acid) on the metal surface. Rossi et al. [15] have combined XPS and ToF–SIMS analyses to study the interaction of dimethylethanolamine (DMEA) on iron surfaces. They concluded that the DMEA molecules were chemisorbed on the oxyhydroxide layer on the iron. A similar approach was attempted by Brundle et al. [16].

In this study, electrochemical measurements (steady-state current–voltage curves and electrochemical impedance spectroscopy) were carried out to characterize and to optimize the inhibitive properties of an original mixture (fatty amines in association with phosphonocarboxylic acid salts and a biocide at low dosage) employed for water treatment in cooling circuits. Its principal advantage being its absence of toxicity. XPS analyses were carried out to determine the chemical composition of the inhibitive film.

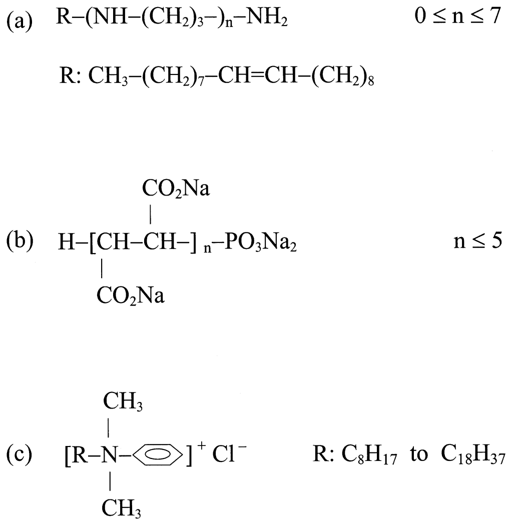

Fig. 1. Chemical structure of the different compounds: (a) oleylaminopropylene amine (fatty amines); (b) phosphonocarboxylic acid salts; and (c) ammonium quaternary salts.

2. Experimental procedure

2.1. *Materials*

The sample selected for the study was an XC 35 carbon steel and had the following composition in percentage by weight: $C \equiv 0.35$, $Mn \equiv 0.65$, $Si \equiv 0.25$, $P \equiv 0.035$, $S \equiv 0.035$ and Fe to 100. For all the experiments, the carbon steel samples were polished with SiC paper down to grade 2400, cleaned in water in an ultrasonic bath and then dried in warm air. The corrosive medium was a 200 mg l^{-1} solution of NaCl (reagent grade) in contact with air maintained at 25 °C. The inhibitor mixture tested was based on oleylaminopropylene amine in association with phosphonocarboxylic acid salts. Quaternary ammonium salts were also present in the mixture. They had a double function: that of dispersing agent and antifouling agent. The structures of the compounds are presented in Figure 1. According to the concentration of the compounds, the pH of the solution varied between 8 and 10. In the inhibitor-free solution, the pH was adjusted to 10 by NaOH.

2.2. *Electrochemical experiments*

The working electrode was a rotating disc consisting of a rod of the carbon steel of 1 cm^2 cross-sectional area, a heat-shrinkable sheath leaving only the tip of the cylinder in contact with the solution. All experiments were carried out at a rotation rate of 1000 rpm. A saturated calomel electrode (SCE) was used as reference and the auxiliary electrode was a platinum grid. The polarization curves were determined potentiostatically with ohmic drop compensation. They were plotted point by point to ensure quasi steady-state conditions. The anodic and the cathodic parts were obtained independently from the corrosion potential after 2 h of immersion. The electrolytic resistance (R_e) was determined from the high-frequency limit of the electrochemical impedance measurements. Electrochemical measurements were carried out using a Solartron 1250 frequency response analyser (frequency range of 65 kHz to a few mHz with eight points per decade) with a Solartron 1286 electrochemical interface. The electrochemical results were obtained from at least three experiments.

2.3. *XPS analysis*

The XPS measurements were carried out on a VG Escalab MKII. The samples were prepared by the same procedure as for the electrochemical experiments (2 h of immersion in the inhibitor-containing solution with a rotation rate of 1000 rpm). Then, the carbon steel sample was removed from the solution, dried in warm air and placed in a vacuum chamber. The specimens were irradiated with a MgK_α ray source. The X-ray power was 300 W. Angle-resolved measurements were made at a take-off angle $\theta = 90°$. The experimental resolution of the binding energy was 1 eV. Sputtering of the sample surface was performed with an argon ion gun under an accelerating voltage of 4 kV and a current density of approximately 75 μA cm^{-2}. After background noise subtraction, peak deconvolution was performed using a least squares fit routine. Binding energies were corrected for charging effects by referencing to the C 1s (284.5 eV) peak. The adsorption of the inhibitive mixture on the steel surface was monitored using the characteristic P 2p, N 1s, and O 1s peaks. The oxidation state of the iron was followed using the Fe 2p signal.

3. Results and discussion

3.1. *Electrochemical results*

The first series of experiments was done to establish the mode of action of the two compounds used separately, that is, if they have an anodic, cathodic or mixed action. Thus, steady-state current–voltage curves and impedance diagrams were obtained in the presence of each compound for different concentrations and compared with the curve obtained in the inhibitor-free solution. The quaternary ammonium salts were added to the amine-containing solution. The QAS concentration was kept constant at 12.5 mg l^{-1}.

3.1.1. *Electrochemical results obtained in the presence of phosphonocarboxylic acid salts (PCAS)*

The polarization curves obtained in the presence of PCAS are presented in Figure 2. A slight shift of the corrosion potential towards more anodic potentials is noted when PCAS was added to the aggressive solution. However, the increase in the PCAS concentration did not change the corrosion potential which remained around −0.4 V vs SCE. In the cathodic range, the curves were independent of the PCAS concentration. A current plateau (800 μA cm^{-2}) appeared from −0.8 to −1.2 V vs SCE, attributed to oxygen reduction [17]. The value of the limiting current density corresponds to that predicted by Levich for a uniformly active surface [18]. In the anodic range, a significant decrease in the anodic current densities was observed when the inhibitor concentration increased. This suggests that PCAS acts only on the anodic sites. For 300 and 400 mg l^{-1} of PCAS a passivity plateau appeared. Its height depended on the inhibitor concentration indicating an improvement of the protective properties of the film when the concentration increased. Around 0 V vs SCE, an abrupt increase of the anodic current density was observed. This increase is associated with the development of localized corrosion. This behaviour is usually observed for anodic inhibitors and is intensified in solutions containing aggressive ions such as chloride. Although the increase of the inhibitor concentration produced a better resistance to uniform corrosion, these concentrations were not sufficient to inhibit localized corrosion. As a matter of fact, for 300 and 400 mg l^{-1} of PCAS, pits appeared at the same potential showing that the number of sites for pitting remained significant. A higher inhibitor concentration would be necessary to induce an increase in the pitting potential.

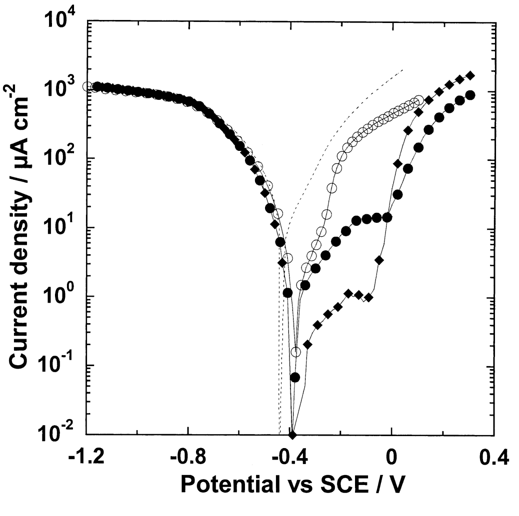

Fig. 2. Steady-state current–voltage curves obtained after 2 h of immersion at E_{corr} for different phosphonocarboxylic acid salt concentrations: (○) 200 mg l^{-1}; (●) 300 mg l^{-1}; (◆) 400 mg l^{-1}; (- - -) blank solution.

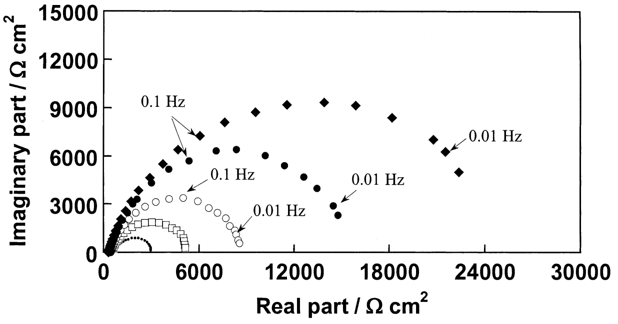

Fig. 3. Electrochemical impedance diagrams obtained after 2 h of immersion at E_{corr} for different phosphonocarboxylic acid salt concentrations: (□) 100 mg l^{-1}; (○) 200 mg l^{-1}; (●) 300 mg l^{-1}; (◆) 400 mg l^{-1}; (- - -) blank solution.

Figure 3 shows the impedance diagrams obtained at the corrosion potential for different PCAS concentrations. With and without inhibitor, the diagrams are characterized by a single time constant. The loop size increased with the increase in salt concentration. Thus, by taking into account the steady-state results, it can be concluded that the impedance diagrams obtained at the corrosion potential are representative of the anodic action of the PCAS. In the literature, different mechanisms have been proposed to explain the inhibitive action of carboxylates. However, it is not clear if the carboxylates react with the iron oxide to form insoluble complexes or if they form a chelate with the metal ions while they are still bound up in the lattice of the metal surface or if they are incorporated into the oxide layer during its formation, plugging the pores [22–24]. Recently, Agarwal and Landolt [11] proposed that the inhibition of metal dissolution is due to the buffer capacity of carboxylates promoting passivation by a blocking mechanism. Indeed, the variation of the interfacial pH is controlled by the amphoteric character of carboxylates and thus, the local pH is maintained in the passivation range which is favoured by oxygen reduction [11, 19–21].

3.1.2. *Electrochemical results obtained in the presence of fatty amines*

Figure 4 shows polarization curves obtained for 10, 25 and 50 mg l^{-1} levels of fatty amines. The corrosion potential was slightly shifted anodically in the presence of fatty amines (FA). Whatever the amine concentration, the curves were weakly dependent on the concentration over the whole potential range studied. A decrease in the cathodic and anodic current densities was observed by comparison with results obtained without inhibitor. This shows that FA act both on the

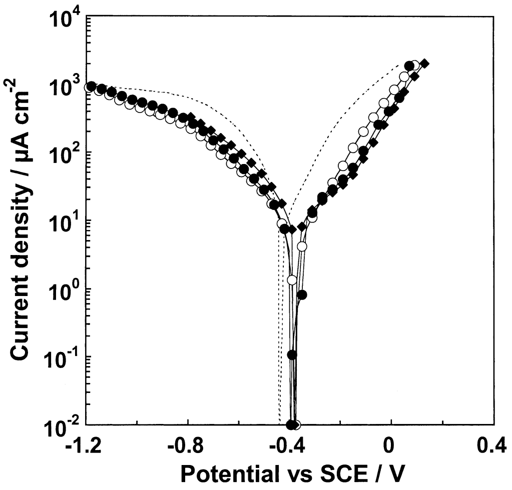

Fig. 4. Steady-state current–voltage curves obtained after 2 h of immersion at E_{corr} for different fatty amine concentrations: (○) 10 mg l^{-1}; (●) 25 mg l^{-1}; (◆) 50 mg l^{-1}; (- - -) blank solution.

cathodic and anodic partial reactions. In the cathodic range, with and without inhibitor, mixed activation and diffusion control occurred near the corrosion potential. Conversely, in the anodic range, active metal dissolution was observed.

Figure 5 shows the impedance diagrams obtained at the corrosion potential for various FA concentrations. The diagrams are characterized by a single capacitive loop. Whatever the concentration, the size of the loop remained the same, corroborating the steady-state results. The distorted shape of the high-frequency part of the diagrams (Figure 5) can be attributed to the formation of a relatively thick and compact protective film on the metal surface in agreement with the previous work of Duprat et al. [4]. However, an immersion time of 2 h would not be sufficient to show the occurrence of a clear loop in the high-frequency domain. The polarization resistance values (R_p) obtained in the presence of FA were lower than those measured in the presence of PCAS. However, the inhibition was significant at low concentrations for FA (10 mg l^{-1}) whereas a higher concentration of PCAS was required to observed the same effect.

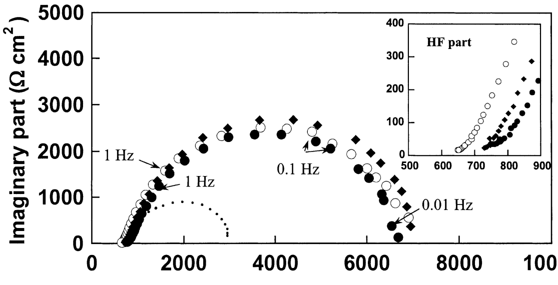

Fig. 5. Electrochemical impedance diagrams obtained after 2 h of immersion at E_{corr} for different fatty amine concentrations: (○) 10 mg l^{-1}; (●) 25 mg l^{-1}; (◆) 50 mg l^{-1}; (- - -) blank solution.

The inhibitive properties of fatty amines in neutral or alkaline media are frequently attributed to their hydrophobic character [25, 34]. In previous studies [26–28], it was shown that there is a relationship between inhibitory efficiency and the hydrophobic properties. An increase in the inhibitory action was observed when the concentration of surfactant in the corrosive solution approaches the critical micellar concentration (CMC). Above this value there was no further increase in efficiency which remained constant for further increases in surfactant concentration. In the present study, our attempts to measure the CMC of oleylaminopropylene amine were unsuccessful probably because it is made up of a mixture of different amines. From the impedance results, it can be assumed that the CMC was below 10 mg l^{-1} because above 10 mg l^{-1}, the diagrams are independent of the concentration. A complementary inhibitive mechanism has also been proposed: the amines interact with the metal ions to form a complex of low solubility providing supplementary blocking [25, 30, 31]. Using the hard and soft acids and bases (HSAB) principle, Aramaki et al. [32] have found that the nitrogen atom is preferentially combined to Fe^{3+}.

3.1.3. *Electrochemical results obtained in the presence of the mixture: fatty amines and phosphonocarboxylic acid salts*

The second series of experiments was performed to find an optimal concentration of fatty amines (FA) and phosphonocarboxylic acid salts (PCAS) in the mixture to combine the action mechanisms of the two compounds used separately. This optimization was done using EIS measurements because in low conductivity medium, the corrosion current densities are frequently overestimated when they are obtained from polarization curves.

Figure 6 shows the impedance diagrams obtained at the corrosion potential for the mixture at different concentrations of FA and PCAS. A minimal concentration of PCAS is desirable in the inhibitive mixture for cost reasons. Thus, 100 mg l^{-1} and 200 mg l^{-1} of PCAS were taken into account for optimization. With the mixture containing 100 mg l^{-1} of PCAS (Figure 6(a)), the polarization resistance increased when the FA concentration increased. The R_p values were higher than that measured in the presence of PCAS alone (100 mg l^{-1}) (Figure 3). Thus, the increase in inhibition effect observed can be attributed to a cooperative adsorption of the two compounds [35]. With the mixture containing 200 mg l^{-1} of PCAS (Figure 6(b)), the polarization resistance values remained constant for 10, 25 and 75 mg l^{-1} of FA. These are close to the value obtained with PCAS alone (200 mg l^{-1}) and higher than the value measured with FA alone (Figure 5). Thus, for these mixtures, it can be assumed that the diagrams are representative of the action of PCAS. When 50 mg l^{-1} of FA was added to 200 mg l^{-1} PCAS, the value of the polarization resistance increased in comparison with PCAS alone. Again, cooperative adsorption of the two compounds was observed. Finally, from Figure 6, it can be observed that

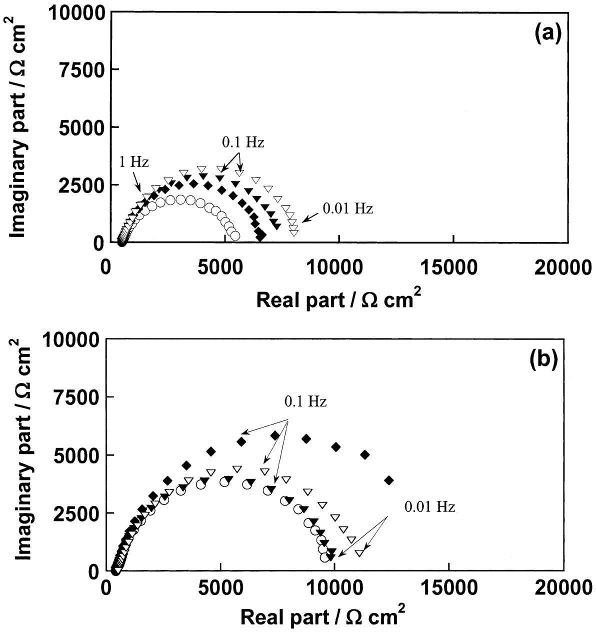

Fig. 6. Electrochemical impedance diagrams obtained after 2 h of immersion at E_{corr} for mixtures composed of (a) 100 mg l^{-1} and (b) 200 mg l^{-1} phosphonocarboxylic acid salts and different fatty amine concentrations: (○) 10 mg l^{-1}; (▼) 25 mg l^{-1}; (◆) 50 mg l^{-1}; (▽) 75 mg l^{-1}.

the highest efficiency was obtained for the mixture: 200 mg l^{-1} PCAS + 50 mg l^{-1} FA. Nevertheless, the role of each component for the different inhibitive mixtures is not clear from the impedance diagrams.

3.1.4. *Quaternary ammonium salt effect in the optimized mixture*

The aim of the third part of this study is to analyse the contribution of quaternary ammonium salt (QAS) in the inhibitive mixture. Figure 7 shows the polarization curves obtained for the carbon steel immersed in 200 mg l^{-1} NaCl, in the presence of the optimized mixture (200 mg l^{-1} PCAS + 50 mg l^{-1} FA) with or without QAS. The concentration of QAS present in the inhibitive mixture was 12.5 mg l^{-1}. Both the anodic and cathodic current densities were slightly decreased and the corrosion potential shifted in the cathodic direction by addition of QAS in the inhibitive mixture. This shows that QAS acted in the inhibition process. The cathodic effect of QAS has already been mentioned for the corrosion of mild steel in acidic solution [29, 33, 34]. Moreover, it has been proposed that the ammonium salts are adsorbed on the metal surface by electrostatic interactions and it was suggested that the presence of halide ions facilitates the adsorption of these cationic compounds [30, 34]. Finally, it is interesting to mention that the anodic curves with and without QAS present the same trend that those obtained with FA alone. This indicates that the susceptibility to localized corrosion of the carbon steel decreased in the presence of the inhibitive mixtures.

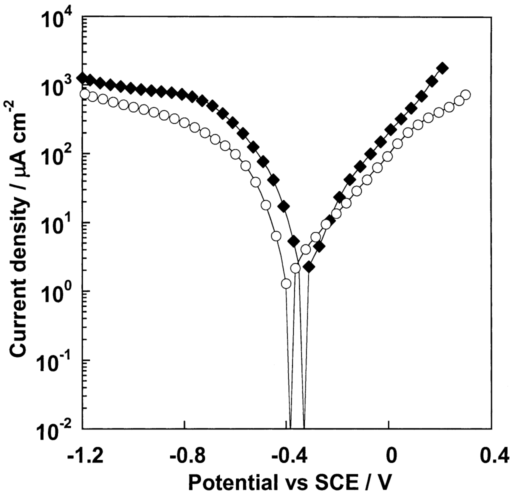

Fig. 7. Steady-state current–voltage curves obtained after 2 h of immersion at E_{corr} for the optimized mixture: (○) with QAS and (◆) without QAS.

3.2. *Surface analysis*

To characterize the initial state of the carbon steel surface before immersion in the solution containing the inhibitive mixture, XPS analysis was performed on a sample just after polishing and cleaning in water in an ultrasonic bath. The general spectrum is presented in Figure 8. It reveals the presence of carbon, oxygen and iron. The C 1s peak at 284.5 eV is attributed to contamination by carbon as mentioned by different authors [36–39]. In the same Figure, the O 1s and Fe 2p regions are enlarged. The O 1s peak is, in fact, composed of two peaks. The peak at 530 eV is related to O^{2-} ion and the other one at 531.6 eV is attributed to the OH^- ion. This suggests that a thin film composed of an iron oxide/hydroxide mixture is present on the metal surface before immersion in the test solution. This is in agreement with the Fe 2p signal composed of a broad peak at 711.8 eV which includes the oxide and metallic states (Figure 8). The same peaks were found by Asami et al. [40] on pure iron left for 24 h in air after mechanical polishing and by Kármán et al. [12] on the carbon steel control surface.

Then, XPS analysis were carried out on the carbon steel surface after 2 h of immersion in the NaCl solution in the presence of the optimized inhibitive mixture. Additionally, argon sputtering was performed to improve analysis of the subsurface of the inhibitive film. Figure 9 presents the high resolution spectra obtained without sputtering (solid line) and after 10 min of sputtering (dashed line) for the different constituents of the inhibitive film. For the P 2p region, before sputtering, a weak signal at 132.1 eV is observed which corresponds to the binding energy of the PO_3^{2-} ion present in the PCAS molecule. This peak was also obtained by several authors studying the interaction between phosphorous compounds and iron [41–43]. After 10 min sputtering, a second peak appeared at 130 eV which can be attributed to the PCAS bonded to the iron oxide substrate [43]. For

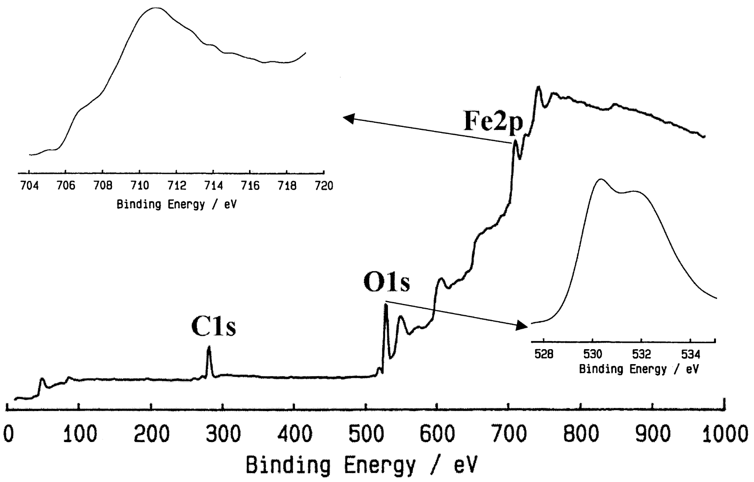

Fig. 8. XPS general spectra of the carbon steel surface.

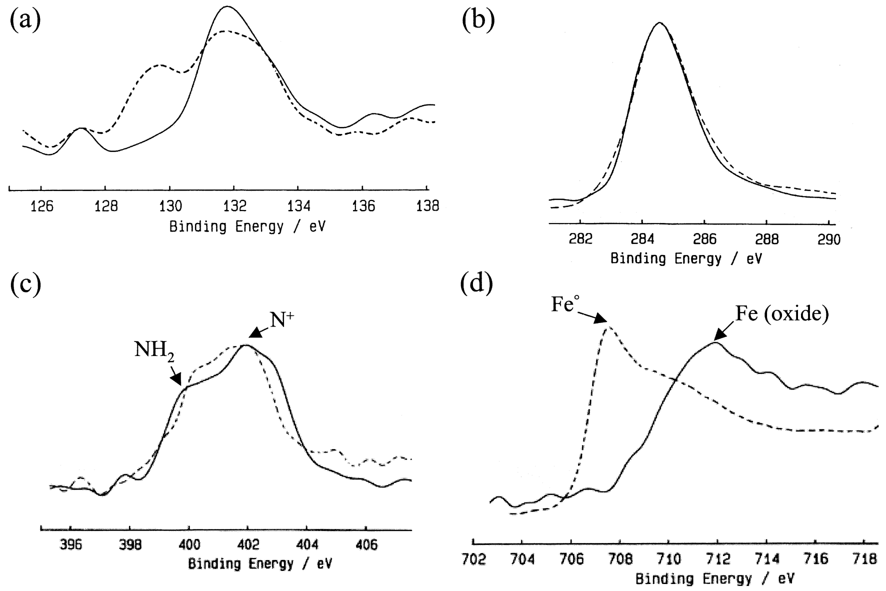

Fig. 9. XPS spectra of (a) P 2p, (b) C 1s, (c) N 1s and (d) Fe 2p for the carbon steel immersed in 200 mg l^{-1} NaCl containing the inhibitive mixture: (—) surface, (- - -) 10 min of sputtering.

the C 1s a single peak at 284.5 eV was identified. This signal is essentially accounted for by the presence of the inhibitor molecules on the steel surface because a large quantity of carbon is measured before and after sputtering. However, as previously mentioned, this peak also includes surface contamination. For the N 1s spectrum (Figure 9(c)), a double peak was obtained. The first peak at 400 eV is attributed to the amine (R–NH$_2$ or R–NH–R) adsorbed on the metal surface. The second one at 402 eV associated with positively charged nitrogen species (R–NH$_3^+$ or R$_4$NCl) and could be associated to the adsorption of the quaternary ammonium salts. To verify this hypothesis, XPS analysis was carried out for two samples immersed in 200 mg l^{-1} NaCl: one, in the presence of 100 mg l^{-1} of amines and the other in the presence of 100 mg l^{-1} quaternary ammonium salts. Figure 10 presents the N 1s scan spectra obtained for the two samples. For the sample treated in the amine-containing solution, the N 1s region is composed of a single peak at 400 eV (Figure 10(a)). The same peak was observed on a carbon steel surface after immersion in a sodium chloride solution containing dimethylethanolamine [15, 39]. Conversely, two peaks can be observed after immersion in the quaternary ammonium salts solution (Figure 10(b)): a peak at 400 eV and another one at 402 eV. The presence of two peaks can be attributed either to the presence of a small quantity of amine in the QAS-containing solution or to the modification of the nitrogen configuration when the QAS were adsorbed on the steel surface [44]. This shows that for the sample immersed in the solution containing the optimized inhibitive mixture, both fatty amine and quaternary ammonium salts are present in the inhibitive layer.

Coming back to the high resolution Fe 2p spectrum (Figure 9(d)), a peak can be observed at 711.8 eV which coincides with the iron oxide/hydroxide mixture. After

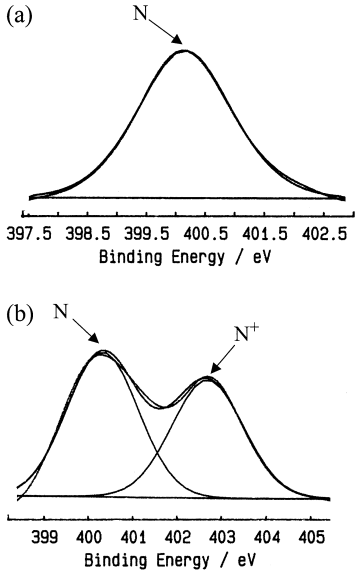

Fig. 10. XPS spectra of the N 1s region for the carbon steel after 2 h of immersion in 200 mg l^{-1} NaCl containing: (a) 100 mg l^{-1} fatty amines, (b) 100 mg l^{-1} quaternary ammonium salts.

10 min of sputtering, the peak of the metal substrate appears at 707.1 eV still in the presence of the oxide/hydroxide signal. Concerning the O 1s spectrum, a broad peak around 532 eV is observed at the surface (Figure 11(a)). Its deconvolution shows the presence of two peaks: one at 531.6 eV and the other at 533.2 eV (Figure 11(b)). The first corresponds to the binding energy of the OH^- ion and the second is often associated in the literature to the presence of water molecules adsorbed on the oxide/hydroxide mixture [12, 13, 40, 45]. After 10 min of sputtering, the O 1s signal is shifted towards lower binding energies (Figure 11(a)). In this case, its deconvolution shows the presence of three peaks (Figure 11(c)): one at 530 eV which corresponds, as shown previously (Figure 8), to the binding energy of the O^{2-} ion and two other peaks at 531.4 eV and at 533.2 eV already observed in Figure 11(b). These three peaks were also observed by Olsson et al. [10] for the adsorption of an aromatic carboxylic acid on a mild steel surface. The presence of water molecules in the iron passivation layer has been discussed by several researchers [46–49]. However, the peak at 533.2 eV also corresponds to the (O=C–) bond which is a functional group of the PCAS molecule. Recent ToF–SIMS experiments with benzoyl alkanoic acid adsorbed on iron suggested strong bonding between the carboxylic inhibitor and the iron surface [50]. Thus, in our case, it is probable that the peak at 533.2 eV reveals the presence of the carboxyl group at the metal surface.

4. Conclusions

Inhibiting the corrosion of a carbon steel by associating fatty amines (FA) with phosphonocarboxylic acid salts (PCAS) was studied with electrochemical measurements and XPS analysis. It was shown that the PCAS act as anodic inhibitors whereas FA act as mixed inhibitors. FA were efficient at low concentrations whereas for PCAS a higher concentration was necessary to reach the same inhibition level. The addition of FA to a PCAS-containing solution improved the carbon steel protection for the mixtures containing the lowest concentration of PCAS (100 mg l^{-1}). Conversely, the FA effect was not significant for the solutions containing the highest concentration of PCAS (200 mg l^{-1}) except for 50 mg l^{-1} of FA where a cooperative adsorption of the two compounds was observed and therefore a maximum efficiency was reached.

From XPS results, we have seen that before immersion in the solution containing the inhibitive mixture,

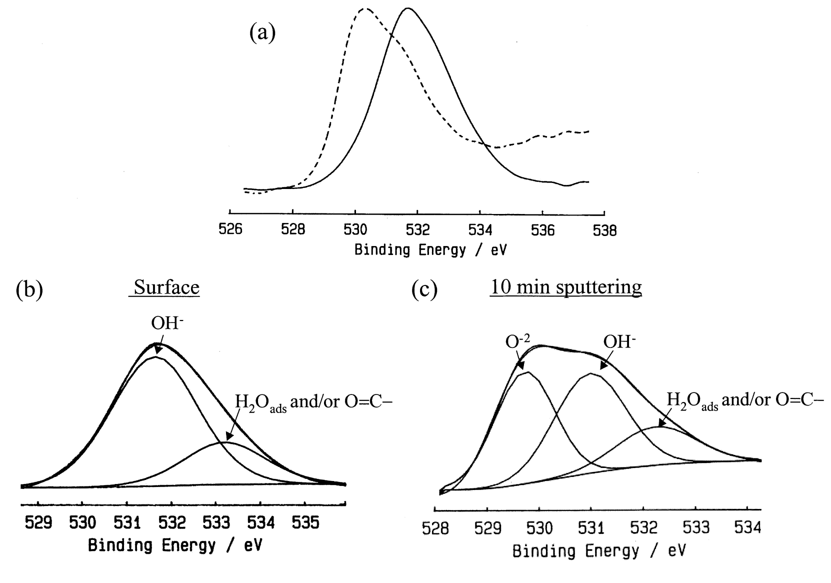

Fig 11. (a) XPS spectra of the O 1s region for the carbon steel after 2 h of immersion in 200 mg l^{-1} NaCl containing the optimized mixture (—) before and (- - -) after 10 min of sputtering. (b) and (c) are the deconvoluted curves.

the carbon steel surface is already covered by an iron oxide/hydroxide mixture. After immersion in the inhibitor-containing solution, these iron oxide/hydroxide mixtures are still present. From the O 1s spectra obtained before and after sputtering, it can be assumed that a thin inner oxide layer covered the steel surface and an outer iron oxide/hydroxide mixture is above it. The inhibitive molecules are seen to be distributed throughout the oxide layers. From the P 2p and N 1s peaks, it was clearly shown that the PCAS, FA and QAS are present in the layer.

For a better understanding of the individual action of FA and PCAS in the inhibitive mixture, it will be interesting to carry out complementary experiments without biocide.

Acknowledgement

The authors wish to express their gratitude to Dr G. Chatainier for fruitful discussions on XPS analysis.

References

1. E. Kálmán, Proc. of 7th European Symposium on 'Corrosion Inhibitors' (7SEIC), Ann. Univ. Ferrara, N. S., Sez. V. Suppl. N.9 (1990), p. 745.
2. I.J. Yang, Proc. (7SEIC), ref. [1], p. 919.
3. M. Duprat, F. Dabosi, F. Moran and S. Rocher, *Corrosion* **37** (1981) 262.
4. M. Duprat, M.C. Lafont, F. Moran and F. Dabosi, *Electrochim. Acta* **30** (1985) 353.
5. M.C. Lafont, N. Pébère, F. Moran and P. Blériot, *Revue des Sciences de L'Eau* **6** (1993) 97.
6. Y. Gonzalez, M.C. Lafont, N. Pébère and F. Moran, *J. Appl. Electrochem.* **26** (1996) 1259.
7. Y. Gonzalez, M.C. Lafont, N. Pébère and F. Moran, Proc. of 8th European Symposium on 'Corrosion Inhibitors' (8SEIC), Ann. Univ. Ferrara, N.S., Sez. V. Suppl. N.10 (1995), p. 453.
8. Y. Gonzalez, M.C. Lafont, N. Pébère, G. Chatainier, J. Roy and T. Bouissou, *Corros. Sci.* **37** (1995) 453.
9. R. Ashcraft, G. Bohnsack, R. Holm, R. Kleinstueck and S. Storp, *Mater. Perform.* **27** (1988) 332.
10. C-O.A. Olsson, P. Agarwal, M. Frey, and D. Landolt, *Corros. Sci.* **42** (2000) 1197.
11. P. Agarwal and D. Landolt, *Corros. Sci.* **40** (1998) 673.
12. F.H. Kármán, E. Kálmán, I. Cserny, J. Telegdi and P. Nagy, *Analusis Magazine* **25** (1997) M33–M34.
13. F.H. Kármán, I. Felhösi, E. Kálmán, I. Cserny and L. Kövér, *Electrochim. Acta* **43** (1998) 69.
14. J.L. Fang, Y. Li, X.R. Ye, Z.W. Wang and Q. Liu, *Corrosion* **49** (1993) 266.
15. A. Rossi, B. Elsener, M. Textor and N.D. Spencer, *Analusis Magazine* **25** (1997) M30–M33.
16. C.R. Brundle, M. Grunze, U. Mäder and N. Blank, *Surf. Interface Anal.* **24** (1996) 549.
17. J.O'M. Bockris and A.K.N. Reddy, 'Modern Electrochemistry' (Plenum, New York, 1970).
18. V.G. Levich, 'Physicochemical Hydrodynamics' (Prentice Hall, Englewood Cliffs, NJ, 1962).
19. Y.I. Kuznetsov, Proc. (7SEIC), ref. [1], p. 11.
20. J.G.N. Thomas, Proc. of 5th European Symposium on 'Corrosion Inhibitors' (5SEIC), Ann. Univ. Ferrara, N. S., Sez. V. Suppl. N.7 (1980), p. 453.
21. A.D. Mercer, Proc. (5SEIC), ref. [20], p. 563.
22. O. Lahodny-Sarc, Proc. (8SEIC), ref. [7], p. 421.
23. R.L. Leroy, *Corrosion* **34** (1978) 98.
24. G. Baril, F. Moran and N. Pébère, Proc. of 9th European Symposium on 'Corrosion Inhibitors' (9SEIC), Ann. Univ. Ferrara, N.S., Sez. V. Suppl. N.11 (2000), p. 849.
25. Y.I. Kuznetsov, 'Organic Inhibitors of Corrosion of Metals' (Plenum, New York, 1996).
26. P. Dupin, A. de Savignac, A. Lattes, B. Sutter and P. Haicour, Proc. (5SEIC), ref. [20], p. 301.
27. P. Dupin, A. de Savignac and A. Lattes, *Mater. Chem.* **6** (1981) 443 and **7** (1982) 549.
28. N. Pébère, M. Duprat, F. Dabosi, A. Lattes and A. de Savignac, *J. Appl. Electrochem.* **18** (1988) 225.
29. F. Dabosi, C. Deslouis, M. Duprat and M. Keddam, *J. Electrochem. Soc.* **130** (1983) 761.
30. G. Trabanelli and V. Carassiti, *in* M.G. Fontana and R.W. Staehle (Eds), '*Corrosion Science and Technology*', Vol. 1 (Plenum, New York, 1970) p. 147
31. J.O'M. Bockris and D.A.J. Swinkels, *J. Electrochem. Soc.* **111** (1964) 736.
32. K. Aramaki and H. Nishihara, Proc. of 6th European Symposium on 'Corrosion Inhibitors' (6SEIC), Ann. Univ. Ferrara, N. S., Sez. V. Suppl. N.8 (1985), p. 67.
33. V.S. Sastri and P.R. Roberge, Proc. 11th International Congress on 'Metallic Corrosion', Florence, Italy, **3** (1990) p. 55.
34. I.L. Rozenfeld, 'Corrosion Inhibitors' (McGraw-Hill, New York, 1981).
35. P. Kern and D. Landolt, *Electrochim. Acta* **47** (2001) 589–598.
36. F. Kardirgan and S. Suzer, *J. Electron. Spect. and Related Phenomena* **114–116** (2001) 597–601.
37. R.D. Boyd, J. Verran, K.E. Hall, C. Underhill, S. Hibbert, R. West, *App. Surf. Sci.* **172** (2001) 135.
38. N. Tsuji, K. Nozawa and K. Aramaki, *Corros. Sci.* **42** (2000) 1523.
39. A. Welle, J.D. Liao, K. Kaiser, M. Grunze, U. Mäder and N. Blank, *Appl. Surf. Sci.* **119** (1997) 185.
40. K. Asami, M.S. De Sa and V. Ashworth, Proc. (6SEIC), ref. [32], p. 773.
41. M.S. Eswaran and P.K. Mathur, *Corros. Sci.* **38** (1996) 1783.
42. M. Koudelka and J. Augustynsky, Proc. (5SEIC), ref. [20], p.1111.
43. D. Schuetzle, R.O. Carter, J. Shyu, R. Dickie, J. Holugka and N. Mc. Intyre, *Appl. Spec.* **40** (1986) 641.
44. D. Kouznetsov, A. Sugier, F. Ropital and C. Fiaud, *Electrochim. Acta* **40** (1995) 1513–1521.
45. E. Buss, I.S. Di Simone, W.S. Chiesa, G. Gusmano, G. Montesperelli and E. Traversa, Proc. (7SEIC), ref. [1], p. 645.
46. J. Kruger, *Corros. Sci.* **29** (1989) 149.
47. N. Sato, K. Kudo and R. Nishimura, *J. Electrochem. Soc.* **123** (1976) 1419.
48. W.E. O'Grady, *J. Electrochem. Soc.* **127** (1980) 555.
49. G.W. Simmons, E. Kellerman and H. Leidheiser, *J. Electrochem. Soc.* **123** (1976) 1276.
50. C.-O.A. Olsson, D. Léonard, P. Agarwal, H-J. Mathieu and D. Landolt, *in* Betrand et al. (Eds) Proc. SIMS XII, 5–10 Sept. 1999, Bruxelles, (Elsevier Science, Amsterdam, 1999).